

UC Irvine

UC Irvine Previously Published Works

Title

Specific heat of Nd_{1-x}CaxB₆ single crystals

Permalink

<https://escholarship.org/uc/item/23z5x72v>

Journal

Physical Review B, 83(11)

ISSN

2469-9950

Authors

Stankiewicz, Jolanta
Evangelisti, Marco
Fisk, Zachary

Publication Date

2011-03-15

DOI

10.1103/physrevb.83.113108

Copyright Information

This work is made available under the terms of a Creative Commons Attribution License, available at <https://creativecommons.org/licenses/by/4.0/>

Peer reviewed

Specific heat of $\text{Nd}_{1-x}\text{Ca}_x\text{B}_6$ single crystals

Jolanta Stankiewicz,^{1,*} Marco Evangelisti,¹ and Zachary Fisk²

¹*Instituto de Ciencia de Materiales de Aragón and Departamento de Física de la Materia Condensada, CSIC–Universidad de Zaragoza, 50009 Zaragoza, Spain*

²*Department of Physics, University of California, Irvine, Irvine, California 92697, USA*
(Received 25 January 2011; published 29 March 2011)

We measured the heat capacity on random alloys of $\text{Nd}_{1-x}\text{Ca}_x\text{B}_6$ ($x < 0.4$) in the 0.4 to 300 K temperature range. We calculated the lattice contribution to the specific heat, arising from the Debye-type phonons of the boron framework and Einstein-type oscillators of the cation sublattice. Subtracting lattice and Schottky-type contributions from the measured heat capacity, we find that the electronic portion, linear in temperature, decreases sharply upon doping with Ca.

DOI: [10.1103/PhysRevB.83.113108](https://doi.org/10.1103/PhysRevB.83.113108)

PACS number(s): 71.27.+a

I. INTRODUCTION

Rare-earth and alkaline-earth metal hexaborides show unusual physical properties, more so if they are synthesized with divalent cations. Their properties can be altered profoundly by slight variations in the band structure, for instance, through doping. For this reason they have been the subject of extensive experimental and theoretical studies for over four decades. Hexaborides exist in the cubic CsCl crystal structure, in which a cage of B_6 octahedra surrounds each cation atom. Compounds with divalent cations are semiconducting. Trivalent cations give rise to metallicity with an estimated one conduction electron per metal atom. Since the hexaborides with different cations remain isostructural, doping studies have been a major component of the experimental work done on these materials. In addition, the strong interaction between the conduction electrons, at low temperatures, makes this class of materials one of the most interesting in the field of strongly correlated electron systems.

Most of the rare-earth hexaborides exhibit some sort of long-range order at low temperatures. The most common is antiferromagnetic (AF) ordering through the Ruderman-Kittel-Kasuya-Yosida (RKKY) exchange interaction, which is strongly influenced by crystal field effects, as is seen in NdB_6 . This compound orders in an A -type collinear antiferromagnetic structure below $T_N \approx 8$ K.¹ The ground state of the Nd^{+3} ions ($J = 9/2$) is split in a cubic crystal field into two Γ_8 quartets and a Γ_6 doublet.^{2,3} The first excited energy is approximately 135 K above the ground Γ_8^2 state, and the nearest Γ_6 excited doublet lies at 278 K.²⁻⁴ A competition between ferro-quadrupolar⁵ and crystalline-electric-field³ (CEF) interactions gives rise to a low-field magnetic anisotropy in NdB_6 which is much weaker than the isotropic magnetic exchange interaction. The topology of the Fermi surface (FS) of NdB_6 has been explored in several works.⁶⁻⁸ It resembles the FS observed in LaB_6 ,⁹ but with additional weak correlations. The FS consists of six large ellipsoids, centered at the X points of the Brillouin zone, which slightly overlap on the ΓMX plane. A simple folding procedure can be used to obtain the AF bands from their paramagnetic counterparts in this hexaboride.¹⁰ In addition, the experimentally found frequency branches of the de Haas-van Alphen effect⁷ can be well reproduced from the calculated Fermi surfaces.¹¹ Band structure calculations also show that 4f levels are rather deep in NdB_6 .¹²

Results of experiments on the thermodynamic properties of NdB_6 have been reported in several papers.^{4,13-17} Magnetic contributions to the specific heat have been found, subtracting the results which had been reported for isostructural LaB_6 . Experimental estimations of the electronic term of the specific heat are scarce and vary from 2 to 80 mJ/K² mol.^{14,15}

In this paper we report heat capacity measurement results for $\text{Nd}_{1-x}\text{Ca}_x\text{B}_6$ alloys, in which some of the trivalent rare-earth atoms are substituted with divalent Ca atoms. We aim to study how a decreasing valence, and the variations in the Fermi surface that follow from it, affect the properties of these alloys. We find that the electronic (linear in temperature) specific heat is moderately enhanced in the paramagnetic region of NdB_6 . It decreases sharply with increasing the content of Ca for $x \lesssim 0.1$.

We describe the experimental procedure in Sec. II. Results of measurements are reported and discussed in Sec. III. Conclusions are drawn in Sec. IV.

II. EXPERIMENT

Single crystals of $\text{Nd}_{1-x}\text{Ca}_x\text{B}_6$ with $x < 0.4$ were grown from stoichiometric amounts of hexaboride components in an Al flux. Crystals grown by this method can often contain flux inclusions or secondary phases within the bulk, or on the surface. We used electron probe analysis to check the composition and homogeneity of the crystals we studied. We found that the Ca and Nd concentrations are spatially uniform over the crystal surfaces. A negligible contamination from Al was seen on some samples. The crystalline structure of alloys was determined by x-ray diffraction.

In our heat capacity experiments, we used small single crystals with an approximate mass of 2 mg. We also measured the heat capacity of a LaB_6 single crystal for a reference purpose. All measurements were performed in a Quantum Design physical properties measurement system (PPMS), with a ³He insert, which enables access to temperatures as low as 0.38 K. A small amount of Apiezon N grease was used in order to hold the crystal in place on a sapphire platform and to assure good thermal contact between the crystal and the platform. The PPMS measures the heat capacity at constant pressure using the relaxation method.

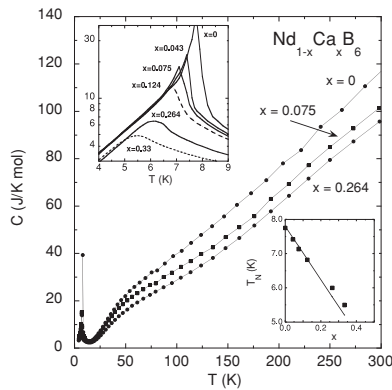


FIG. 1. Plots of C vs T for $\text{Nd}_{1-x}\text{Ca}_x\text{B}_6$ single crystals. A blowup of the transition region is shown in the upper inset. The solid and dashed lines are guides to the eye. The variation of the critical temperature with x is displayed in the lower inset. The solid line is the expected variation (see text).

III. RESULTS AND DISCUSSION

How the zero-field specific heat C , obtained for several $\text{Nd}_{1-x}\text{Ca}_x\text{B}_6$ single crystals, varies with temperature T in the range from 0.4 to 300 K is shown in Fig. 1. The sharp peaks in the $C(T)$ curves come from the antiferromagnetic phase transition; for NdB_6 , $T_N = 7.7$ K. Upon doping with Ca, the peak at T_N shifts to lower temperatures and becomes smaller with a larger high-temperature tail. This is shown in the inset of Fig. 1. The variation of the critical temperature with x can easily be explained within the frame of molecular field theory for which T_N is linearly proportional to the number n_{Nd} of nearest magnetic neighbors for each Nd^{3+} ion. Since the inclusion of calcium causes a change in n_{Nd} , the shift of the ordering temperature is expressed as $T_N(\text{Nd}_{1-x}\text{Ca}_x\text{B}_6) = (1-x)T_N(\text{NdB}_6)$. The lower inset of Fig. 1 shows that the agreement between the observed and expected (from the above relation) ordering temperatures is very good.

Generally, there are electronic, magnetic, and phonon contributions to the specific heat $C(T)$, i.e., $C(T) = C_{\text{el}} + C_{\text{mag}} + C_{\text{ph}}$. In order to analyze the electronic C_{el} and magnetic C_{mag} parts of the specific heat, we need to model and then subtract from the total heat capacity the phonon contribution C_{ph} . The latter was calculated using a model, first proposed by Mandrus and collaborators¹⁸ for hexaborides, that treats the rare-earth or other metal ions as independent harmonic (Einstein) oscillators embedded in a Debye bath of boron ions. This follows from the observation that the metal ions are weakly bound in hexaborides but strong covalent bonds between boron atoms give rise to a very rigid boron sublattice. To check the applicability of this model, we have compared its predictions to the experimental data which we have obtained for the heat capacity of a LaB_6 single crystal in a temperature range 0.3–40 K. Values of 140 and 1160 K has been assumed for the Einstein and Debye temperature, respectively. These values follow from corresponding atomic displacements parameters.¹⁸ As shown in Fig. 2, the agreement between experimental and calculated heat capacity is nearly perfect, assuming a small electronic term of 0.002 J/mol K^2 .

To proceed with calculations of the phonon contribution in $\text{Nd}_{1-x}\text{Ca}_x\text{B}_6$ alloys, we estimate the Einstein temperature T_E

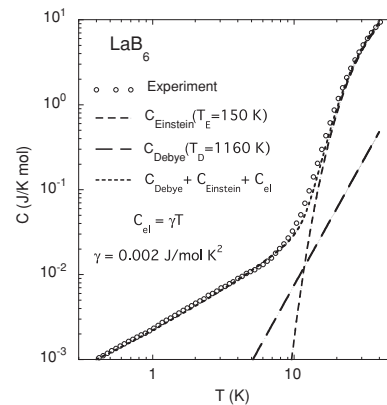


FIG. 2. Specific heat per mole of LaB_6 vs temperature and model calculations performed as described in the text.

of the Nd and Ca atoms from their atomic displacement parameters at room temperature.^{18–21} We used values of 150 and 280 K for T_E of Nd and Ca, respectively. These are very close to the values which one obtains by renormalization of $T_E(\text{La})$ by the square root of the corresponding mass ratio. An examination of x-ray refinements implies a Debye temperature of approximately 1300 K for the simple cubic B_6 lattice in NdB_6 .²⁰ The lattice specific heat is now given by $C_{\text{ph}} = C_{\text{ph}}(\text{Debye}) + xC_{\text{ph}}(\text{Einstein, Ca}) + (1-x)C_{\text{ph}}(\text{Einstein, Nd})$; six moles of B ions are treated as a Debye solid and $1-x$ (x) moles of Nd (Ca) ions as Einstein oscillators. How these terms depend on temperature for $\text{Nd}_{1-x}\text{Ca}_x\text{B}_6$ alloys is shown in Fig. 3. The Debye term is, as expected, very small at low temperatures, and only the Einstein contribution is significant for $T \gtrsim 10$ K.

We now turn to the electronic and magnetic specific heat. Away from the phase transition, in the paramagnetic region, $C_{\text{mag}} \approx C_{\text{Sch}}$, where C_{Sch} is the Schottky contribution, brought about by the CEF splitting of the Nd^{3+} levels. This can be straightforwardly calculated from the known parameters.^{2–4} After Ref. 4, we use a value of 100 K for the first excited energy

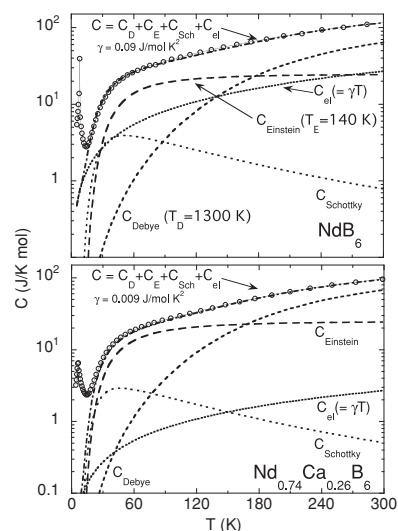


FIG. 3. Specific heat per mole of NdB_6 and $\text{Nd}_{0.74}\text{Ca}_{0.26}\text{B}_6$ vs temperature and model calculations performed as described in the text.

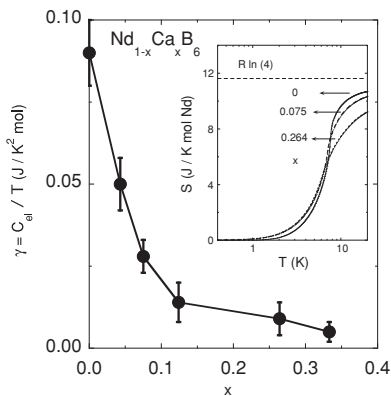


FIG. 4. Coefficient of the electronic specific heat γ vs content of Ca in $\text{Nd}_{1-x}\text{Ca}_x\text{B}_6$ single crystals. The variation of magnetic entropy S vs T for some $\text{Nd}_{1-x}\text{Ca}_x\text{B}_6$ single crystals is shown in the inset.

above the ground Γ_8^2 state, and a value of 278 K for the higher-lying excited doublet. We then assume that the Schottky contribution scales linearly with x ; i.e., $C_{\text{Sch}} = (1-x)C_{\text{Sch}}(\text{NdB}_6)$. To fit experimental data, we need in addition the electronic term, whose linear in T contribution is also shown in Fig. 3 for the $x = 0$ and 0.26 alloys. We obtain a value of 90 ± 10 mJ/K² mol for γ in NdB_6 ($C_{\text{el}} = \gamma T$), in good agreement with previously reported experimental¹⁴ and calculated²² values. We note that this value of γ , in the free-electron-gas model, leads to an effective mass of about $50m_e$ (m_e is the free-electron mass), which is much larger than the effective masses that follow from de Haas–van Alphen experiments.^{7,8} It may happen that the Fermi surface is made up of two distinct sets of bands and only a FS sheet with a light mass is observed in de Haas–van Alphen experiments. Such a situation has been proposed to explain a similar discrepancy in CeB_6 .²³ We also note that de Haas–van Alphen measurements are performed in high magnetic field, so the effective masses may be small.

A linear fit to the data points $C_{\text{el}} = C(T) - C_{\text{Sch}} - C_{\text{ph}}$ in the temperature range from approximately 25 to 300 K for $x = 0, 0.075$, and 0.264, and in the range from 25 to 40 K for $x = 0.043, 0.124$, and 0.33, gives the variation of $\gamma(x)$ which is displayed in Fig. 4 with the corresponding error bars. The coefficient of the electronic specific heat decreases sharply upon alloying of NdB_6 with Ca, for $x \lesssim 0.1$. Our previous Hall effect measurements on $\text{Nd}_{1-x}\text{Ca}_x\text{B}_6$ showed that the carrier concentration n decreases linearly with x .²⁴ Knowing n , we can compare the value of $\gamma(x)$ obtained from the present specific heat measurements with those expected from the Sommerfeld model of the free-electron gas, in which $\gamma = \pi^2 n k_B^2 m^* / \hbar^2 k_F^2$. Here, k_B is the Boltzmann constant, m^* is the effective mass of carriers, and k_F is the Fermi momentum, given by $k_F = (3\pi^2 n)^{1/3}$, which yields the relation $\gamma \propto m^* n^{1/3}$. It is clear that $\gamma(x)$ does not follow an $n^{1/3}$ dependence, which suggests that m^* decreases nonlinearly with increasing Ca content. Interestingly, the anomalous contribution to the Hall effect in $\text{Nd}_{1-x}\text{Ca}_x\text{B}_6$ single crystals shows a similar, strongly nonlinear variation upon doping with Ca.²⁴ Such behavior may arise from drastic alterations of the Fermi surface upon doping.

A log-log plot of $C(T)/T$ in the ordered state is shown in Fig. 5 for two single crystals. Below 0.6 K, the experimental

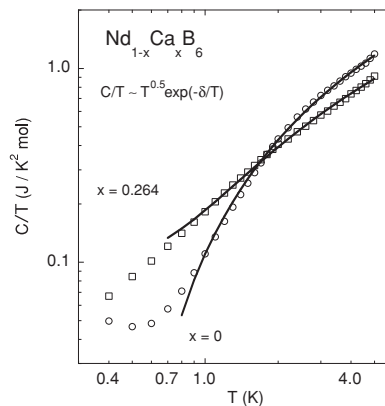


FIG. 5. Log-log plot of C/T vs T for NdB_6 and $x = 0.264$ single crystals.

heat capacity increases slightly toward 0.3 K owing to the hyperfine splitting of the Nd and B nuclei's magnetic levels.^{25,26} We tried to fit the heat capacity in the ordered state using expressions for magnetic spin waves. However, we failed to find a reasonable fit. The solid lines in Fig. 5 show how the heat capacity, arising from gapped ferromagnetic spin waves and given by $(C - C_{\text{hf}})/T \propto T^n \exp(-\delta/k_B T)$, where C_{hf} is the hyperfine contribution, k_B is the Boltzmann constant, δ is the spin wave energy gap, and $n = 0.5$,²⁷ fits experimental points in the ordered state. The quality of the fit is poor for temperatures below 1 K.

To obtain the magnetic entropy S , shown in the inset of Fig. 4, we use the relation $S(T) = \int_0^T dT (\Delta C_{\text{mag}}/T)$, where ΔC_{mag} is the remainder of the total heat capacity after the hyperfine, phonon, Schottky, and electronic contributions have been subtracted. The calculated entropy is therefore associated only with the magnetic ordering. We used values of γ shown in Fig. 4 below T_N . This agrees with the observation that neither the number of electrons contained in the Fermi surface nor the effective mass changes significantly going from the paramagnetic phase at higher temperatures to the antiferromagnetic phase at lower temperatures. Our estimate of S indicates that about 85% of the spin entropy, associated with the ground quartet [$R \ln(4)$, where R is the gas constant], per mole at T_N expected for trivalent Nd is accounted for at $x = 0$. The value of magnetic entropy at T_N agrees well with the results of earlier studies on the same system^{17,28} and with the theoretical predictions.²⁹ Correlation ranges decrease gradually as T increases beyond T_N , and, consequently, S also increases gradually.

IV. CONCLUDING REMARKS

The experimentally found heat capacity of $\text{Nd}_{1-x}\text{Ca}_x\text{B}_6$ single crystals is fitted by a simple model in which lattice and magnetic contributions are assumed to scale linearly with the content of Ca. Remarkably, with the above assumption we were able to fit experimental data in a wide temperature and composition range. This shows that the RB_6 structure does not deform much when a trivalent R is replaced by a divalent one, as expected for the rigid covalently bonded boron network. Although the Raman scattering spectra of hexaborides

show slight variations upon doping with divalent elements,³⁰ these seem not to affect significantly the phonon and CEF parameters in the alloys studied. Our results show a moderate enhancement of the electronic part in $x = 0$ alloys in both the paramagnetic and antiferromagnetic phases. Interestingly, the low-temperature magnetic resistivity of NdB₆ is also strongly enhanced with respect to the usual values of electron-magnon scattering in magnetic metals.³¹ This points to an important role of electronic correlations in this material.

Upon doping with Ca, the electronic term in the specific heat of Nd_{1-x}Ca_xB₆ in the paramagnetic phase decreases sharply, and, for $x \gtrsim 0.1$, shows values expected for magnetic metals. The electronic properties of hexaborides depend critically on details of the band structure in the vicinity of the X point. In NdB₆, the electron ellipsoids centered at the X point of the Brillouin zone slightly overlap and small necks are formed between them. Doping of NdB₆ with a divalent element lowers the electron concentration. Consequently, the volume of the electron ellipsoids decreases and the overlap between them, as well as the interconnecting necks, may disappear. The behavior of γ with Ca concentration is perhaps what one might expect if the electron ellipsoids become separated and the large value of the electronic heat capacity is coming from the Fermi surface

necks. This would explain the main features of the electronic properties we have observed.

An alternative explanation would involve effects of quadrupolar interactions which are apparently important in NdB₆.³ Quadrupole related effects lead to the exotic behavior found in the filled skutterudites, and, in particular, to a large electronic specific heat.³² The large value of γ in NdB₆ ($C_{el} = \gamma T$) could be related to similar interactions. Then, the strain fields that arise when Ca is doped into NdB₆ lift the degeneracy of the ground state quartet of the Nd ion. Quadrupole interactions are strongly reduced and, consequently, $\gamma(x)$ decreases. Further experimental and theoretical studies would be very helpful at this point.

ACKNOWLEDGMENTS

We are happy to acknowledge support from Grant No. MAT2008-03074 and No. MAT2009-13977-C03, from the Ministerio de Ciencia e Innovación of Spain, and from National Science Foundation Grant No. DMR-0854781. Additional support from Diputación General de Aragón (DGA-IMANA) is also acknowledged. We thank S. Nakatsuji and A. D. Bianchi for growing the single crystals used in this study.

*jolanta@unizar.es

¹C. M. McCarthy and C. W. Tompson, *J. Phys. Chem. Solids* **41**, 1319 (1980).

²M. Loewenhaupt and M. Prager, *Z. Phys. B: Condens. Matter* **62**, 195 (1986).

³G. Uimin and W. Brenig, *Phys. Rev. B* **61**, 60 (2000).

⁴M. Reiffers, J. Šebek, E. Šantavá, N. Shitsevalova, S. Gabáni, G. Pristáš, and K. Flachbart, *J. Magn. Magn. Mater.* **310**, e595 (2007).

⁵M. Sera, S. Itabashi, and S. Kunii, *J. Phys. Soc. Jpn.* **66**, 548 (1997).

⁶A. P. J. van Deursen, Z. Fisk, and A. R. de Vroomen, *Solid State Commun.* **44**, 609 (1982).

⁷Y. Onuki, A. Umezawa, W. K. Kwok, G. W. Crabtree, M. Nishihara, T. Yamazaki, T. Omi, and T. Komatsubara, *Phys. Rev. B* **40**, 11195 (1989).

⁸R. G. Goodrich, N. Harrison, and Z. Fisk, *Phys. Rev. Lett.* **97**, 146404 (2006).

⁹A. P. J. Arko, G. Crabtree, D. Karim, F. M. Mueller, and L. R. Windmiller, *Phys. Rev. B* **13**, 5240 (1976)

¹⁰B. I. Min and Y. -R. Jang, *Phys. Rev. B* **44**, 13270 (1991).

¹¹Y. Kubo, S. Asano, H. Harima, and A. Yabase, *J. Phys. Soc. Jpn.* **62**, 205 (1993).

¹²M. Kitamura, *Phys. Rev. B* **49**, 1564 (1994).

¹³Z. Fisk, *Solid State Commun.* **18**, 221 (1976).

¹⁴N. N. Sirota, V. V. Novikov, and S. V. Antipov, *Phys. Solid State* **39**, 815 (1997).

¹⁵V. V. Novikov, *Phys. Solid State* **43**, 300 (2001).

¹⁶E. F. Westrum, J. T. S. Andrews, B. H. Justice, and D. A. Johnson, *J. Chem. Thermodyn.* **34**, 239 (2002).

¹⁷S. Tsuji, T. Endo, S. Kobayashi, Y. Yoshino, M. Sera, and F. Iga, *J. Phys. Soc. Jpn.* **71**, 2994 (2002).

¹⁸D. Mandrus, B. C. Sales, and R. Jin, *Phys. Rev. B* **64**, 012302 (2001).

¹⁹Ya. I. Dutchak, Ya. I. Fedysheyn, Yu. B. Paderno, and D. I. Vadets, *Izv. Vyssh. Uchebn. Zaved., Fiz.* **1**, 154 (1973).

²⁰M. K. Blomberg, M. J. Merisalo, M. M. Korsukova, and V. N. Gurin, *J. Alloys Compd.* **217**, 123 (1995).

²¹M. M. Korsukova, V. N. Gurin, T. Lundstrom, and L. E. Tergerius, *J. Less-Common Met.* **117**, 73 (1986).

²²H. D. Langford, W. M. Temmerman, and G. A. Gehring, *J. Phys.: Condens. Matter* **2**, 559 (1990).

²³Y. Onuki, T. Komatsubara, P. H. P. Reinders, and M. Springford, *Physica B* **163**, 100 (1990).

²⁴J. Stankiewicz, A. D. Bianchi, and Z. Fisk, *J. Phys.: Conf. Ser.* **200**, 012192 (2010).

²⁵C. D. Bredl, *J. Magn. Magn. Mater.* **63-64**, 355 (1987).

²⁶A. C. Anderson, B. Holmström, M. Krusius, and G. R. Pickett, *Phys. Rev.* **183**, 546 (1969).

²⁷E. S. R. Gopal, *Specific Heats at Low Temperatures* (Plenum, New York, 1966).

²⁸S. Kobayashi, M. Sera, M. Hiroi, N. Kobayashi, and S. Kunii, *J. Phys. Soc. Jpn.* **68**, 3407 (1999).

²⁹L. J. de Jongh and A. R. Miedema, *Adv. Phys.* **50**, 947 (2001).

³⁰N. Ogita, S. Nagai, N. Okamoto, M. Udagawa, F. Iga, M. Sera, J. Akimitsu, and S. Kunii, *Phys. Rev. B* **68**, 224305 (2003).

³¹J. Stankiewicz, S. Nakatsuji, and Z. Fisk, *Phys. Rev. B* **71**, 134426 (2005).

³²Y. Aoki, H. Sugawara, H. Hisatomo, and H. Sato, *J. Phys. Soc. Jpn.* **74**, 209 (2005).